3586 *Chem. Mater.* **2009,** *21,* 3586–3592
DOI:10.1021/cm900624z

CHEMISTRY OF MATERIALS
Article

Microwave Synthetic Route for Highly Emissive TOP/TOP-S Passivated CdS Quantum Dots

Aaron L. Washington, II, and Geoffrey F. Strouse*

Department of Chemistry and Biochemistry, Florida State University, Tallahassee, Florida 32306-4390

Received March 4, 2009. Revised Manuscript Received June 3, 2009

Through selective microwave absorption, we demonstrate the ability to activate TOPS as an efficient sulfur donor, allowing the rapid (18 m) growth of highly emissive (PLQY = 33%), Zn blende CdS quantum dots (QDs) passivated by TOP/TOPS in the 4−6 nm size regime (5% size dispersity). The CdS QDs exhibit sharp absorption features and bandedge photoluminescence even for the largest CdS sample. Addition of hexadecylamine restricts the growth rate by limiting the Cd monomer activity and lowers overall PLQY. The use of MW chemistry for QD formation allows a highly reproducible synthetic protocol that is fully adaptable to industrial applications.

Introduction

The development of II−VI semiconductor quantum dots (QDs) has expanded exponentially over the last 15 years due largely to advancements in reactive monomers and the QD growth conditions.[1−9] Recent studies have definitively correlated growth and dispersity for the QDs to the reaction operating in the diffusion-controlled or reaction-controlled mechanism, depending upon the heating conditions and addition of additives.[10−19] Under conditions where slow release of the chalcogenide from the solution phase monomer is achieved, the reaction proceeds predominately through a diffusion controlled mechanism, and thus the size dispersity is controlled by monomer concentration, in effect the equilibrium that exists between monomer bound to the QD surface and free in solution.[20] Although these efforts have clearly identified organic additives that manipulate the diffusion-controlled reaction rates via controlling surface activity, little effort has focused on the activation of monomers directly through the use of selective energy absorption into the specific monomer. In a series of studies, we have explored the use of selective MW absorption into tri-*n*-alkyl phosphine complexes of the form R_3P-X (R = alkyl, X = Se, Te) leading to remarkable enhancements of reaction rates for QD formation.[21] The realization that selective absorption can enhance the activity of the TOP-Se or TOP-Te monomer in a solvothermal reaction conducted in a MW cavity suggests that monomers with low activity might be enhanced by the absorption of MW energy.

Although there is a plethora of examples of CdSe and CdTe materials generated from R_3P-X, it is surprising that there are no reports of growing CdS form R_3P-S as a precursor without the addition of alkyl phosphonic acids to enhance reaction rates, although TOP-S is a common reagent for the shelling step in a core−shell QD.[10,12,19,22,23] Because nearly all the published II−VI metal chalcogenide nanocrystals are readily prepared from R_3P-X, the limited examples of CdS prepared from TOPS is surprising although it can be traced to the bond strength of P−S

*Corresponding author. E-mail: Strouse@chem.fsu.edu.

(1) Rossetti, R.; Ellison, J. L.; Gibson, J. M.; Brus, L. E. *J. Chem. Phys.* **1984**, *80*(90), 4464.
(2) Empedocles, S. A.; Norris, D. J.; Bawendi, M. G. *Phys. Rev. Lett.* **1996**, *77*(18), 3873–3876.
(3) Mews, A.; Eychmueller, A.; Giersig, M.; Schooss, D.; Weller, H. *J. Phys. Chem.* **1994**, *98*(3), 934–41.
(4) Rajh, T.; Micic, O. I.; Nozik, A. J. *J. Phys. Chem.* **1993**, *97*(46), 11999–2003.
(5) Micic, O. I.; Curtis, C. J.; Jones, K. M.; Sprague, J. R.; Nozik, A. J. *J. Phys. Chem.* **1994**, *98*(19), 4966–9.
(6) Peng, Z. A.; Peng, X. *J. Am. Chem. Soc.* **2001**, *123*(1), 183–184.
(7) Dabbousi, B. O.; Rodriguez-Viejo, J.; Mikulec, F. V.; Heine, J. R.; Mattoussi, H.; Ober, R.; Jensen, K. F.; Bawendi, M. G. *J. Phys. Chem. B* **1997**, *101*(46), 9463–9475.
(8) Xi, L.; Tan, W. X. W.; Boothroyd, C.; Lam, Y. M. *Chem. Mater.* **2008**, *20*(16), 5444–5452.
(9) Talapin, D. V.; Rogach, A. L.; Shevchenko, E. V.; Kornowski, A.; Hasse, M.; Weller, H. *J. Am. Chem. Soc.* **2002**, *124*(20), 5782–5790.
(10) Peng, A. Z.; Peng, X. G. *J. Am. Chem. Soc.* **2002**, *124*, 3343.
(11) Lui, H.; Owen, J. S.; Alivisatos, A. P. *J. Am. Chem. Soc.* **2007**, *129* (2), 305–312.
(12) Cao, Y. C.; Wang, J. *J. Am. Chem. Soc.* **2004**, *126*, 14336–14337.
(13) Mohamed, M. B.; Tonti, D.; Al-Salman, A.; Chemseddine, A.; Chergui, M. *J. Phys. Chem. B* **2005**, *109*(21), 10533–10537.
(14) Murray, C. B.; Norris, D. J.; Bawendi, M. G. *J. Am. Chem. Soc.* **1993**, *115*, 8706.
(15) Manna, L.; Scher, E. C.; Alivisatos, A. P. *J. Am. Chem. Soc.* **2000**, *122*, 12700.
(16) Rogach, A. L.; Kornowski, A.; Gao, M. Y.; Eychmuller, A.; Weller, H. *J. Phys. Chem. B* **1999**, *103*, 3065.
(17) Vossmeyer, T.; Katsikas, L.; Giersig, M.; Popovic, I. G.; Diesner, K.; Chemseddine, A.; Eychmuller, A.; Weller, H. *J. Phys. Chem.* **1994**, *98*, 7665.
(18) Qu, L. H.; Peng, X. G. *J. Am. Chem. Soc.* **2002**, *124*, 2049.
(19) Yu, W. W.; Wang, Y. A.; Peng, X. G. *Chem. Mater.* **2003**, *15*, 4300.
(20) Talapin, D. V.; Rogach, A. L.; Haase, M.; Weller, H. *J. Phys. Chem. B.* **2001**, *105*(49), 12278–12285.
(21) Washington, A. L., II; Strouse, G. F. *J. Am. Chem. Soc.* **2008**, *130* (28), 8916–8922.
(22) Talapin, D. V.; Nelson, J. H.; Shevchenko, E. V.; Aloni, S.; Sadtler, B.; Alivisatos, A. P. *Nano Lett.* **2007**, *7*(10), 2951–2959.
(23) Shieh, F.; Saunders, A. E.; Korgel, B. A. *J. Phys. Chem. B.* **2005**, *109*(18), 8538–8542.

Published on Web 07/10/2009

(444 ± 8 kJ/mol), P−Se (364 ± 10.0 kJ/mol), vs P−Te (280 ± 10.0 kJ/mol).[24] Consistent with this observation, a more typical sulfur monomer is TMS-S because of its greater monomer activity reflecting the weaker Si−S bond strength relative to P−S.[14] The strength of the P−S interaction limits the ability for TOP-S to act as a good monomer for sulfur addition to the growing QD, thus impacting the ability to form a stable critical nuclei in solution.[2,5,12] Because the bond strength controls the monomer activity ($E_{P-S} > E_{P-Se} > E_{P-Te}$), it directly influences the growth rates for the II−VI nanocrystals (dr/dt(CdTe) > dr/dt(CdSe) > dr/dt(CdS)). Thus it is not surprising that few examples of formation of CdS from R_3P -S exist unless an activator is added to enhance the monomer activity of TOPS leading to materials that exhibit narrow size dispersity, well-defined excitonic absorption features, and strong bandedge photoluminescence at large CdS sizes.[25,26]

The low sulfur atom transfer efficiency in R_3P-S may be enhanced in this reaction if bond cleavage can be activated in the monomer through selectively energizing the monomer. In a lyothermal reaction this is impossible to achieve; however, in a microwave (MW) reaction selective absorption of MW energy can enhance reaction rates by overcoming kinetic barriers in the reaction.[27] It has been shown in both organic chemistry and nanomaterial chemistry that MW absorption is selective into the free solution monomer with the highest static dipole moment if the reactions are carried out in a solution that has a very low MW absorption cross-section.[28] In the QD reactions, whether the rate enhancement arises from local heating in the heterogeneous reaction environment or from selective activation of the monomer is still unknown.

In this manuscript, we report selective absorption of microwave (MW) energy into TOPS leads to formation of 4−6 nm CdS quantum dots (QD) with narrow size dispersity (5% rms based on TEM). The CdS QDs reported herein exhibit an aspect ratio of 1.2 with a size dispersity of 5%, discrete excitonic features in the absorption spectra, band edge photoluminescence (PL), and the highest reported quantum yields (33% PLQY). Defect PL, arising from glide plane defects and/or vacancies, constitutes less than 5% of the total observed emission. The highest bandedge PLQY (PLQY = 33%) is achieved for the 4.3 nm CdS carried out at a 1:1 molar TOP:HDA ratio. The high PLQY is remarkable when compared to earlier reports, where the PLQY is typically less than 20%.[29,30] Consistent with the bond strength argument, the formation of CdS requires much longer reaction times (18 min) than observed previously for formation of CdSe (30 s) or CdTe (15 s) even with MW assisted activation of R_3P-S. The restricted growth behavior of CdS grown in the presence of HDA is believed to reflect a reduced monomer and QD surface activity limiting the burst growth achieved by selective MW absorption into the R_3P-S monomer, thus limiting Cd monomer activity and growth rates of the QD resulting in the observed increased size distributions and higher defect densities.

Experimental Section

Chemicals. All reactants and solvents were used without further purification. Cadmium stearate (CdSA, 90%) and sulfur powder (S, 99.99%) were purchased from Strem Chemicals. Cadmium stearate is a known carcinogen. Tri-*n*-octylphosphine (TOP, 90%) was purchased from Alfa Aesar. Decane (99%) was purchased from Acros Organics.

Characterization. The CdS QDs are analyzed for size (cross-correlated to TEM) and crystal structure by powder X-ray Diffraction (pXRD). The size of the QD is fit by utilizing the Scherrer expression[31]

$$D = \frac{b\lambda}{\Delta(2\theta)\cos\theta}$$

where D is the QD diameter, b is shape coefficient (b is a shape factor of the particle and in this study is set to a value of 1.1 based on correlation of the TEM and pXRD sizing), λ is the wavelength of the X-ray radiation source (Cu Kα 1.5418 Å), $\Delta(2\theta)$ is the full width at half-maximum (fwhm) in 2θ, and θ is the angle for the pXRD peak. Correlation of the pXRD to absorption spectra and select TEM indicates the Scherrer analysis adequately predicts the size. TEM imaging of selected sizes is used to estimate the size dispersity.

Room temperature pXRD were recorded on 10 mg powdered samples on a Rigaku DMAX 300 Ultima 3 Powder X-ray diffractometer (using Cu Kα, λ = 1.5418 Å radiation). The pXRD is calibrated to Si°. Transmission electron microscopy (TEM) obtained using a Philips CM 300-field emission gun with a maximum acceleration voltage of 300 keV. A Gatan 673 wide angle CCD camera with a field of view of 49 mm × 49 mm was used to digitize the micrographs. TEM samples were prepared as dilute solutions in toluene with an absorbance of less than 0.1 to prevent aggregation. One drop of the prepared solution was placed onto a holey carbon 400 mesh TEM grid for 1 min and the drop was removed. The TEM sample was dried overnight in a desiccator prior to imaging. The *d*-spacing for the observable fringes were analyzed using a calibrated TEM to lattice spacing in Au.

Optical experiments were performed on 1×10^{-9} M CdS dissolved in toluene. Absorption measurements were performed on a Varian Cary 50 UV−vis spectrophotometer. Photoluminescence measurements were performed on a Varian Cary Eclipse Fluorescence spectrophotometer using quartz cuvettes (cell path length = 1 cm).

Synthesis. All syntheses were performed in a single mode CEM Discover System operating at 300W, 2.45 GHz. The

(24) Drowart, J.; Myers, C. E.; Szwarc, R; Vander Auwera-Mahieu, A.; Uy, O. M. *High Temp. Sci.* **1973**, *5*, 482.
(25) Yu, W. W.; Peng, X. *Angew. Chem., Int. Ed.* **2002**, *41*(13), 2368–2371.
(26) Karan, S.; Malik, B. *J. Phys. Chem. C* **2007**, *111*(45), 16734–16741.
(27) De La Hoz, A.; Diaz-Ortiz, A.; Moreno, A. *Curr. Org. Chem.* **2004**, *8*(10), 903–918.
(28) de la Hoz, A.; Diaz-Ortiz, A.; Moreno, A. *Chem. Soc. Rev.* **2005**, *34* (2), 164–178.
(29) Steckel, J. S.; Zimmer, J. P.; Coe-Sullivan, S.; Stott, N. E.; Bulovic, V.; Bawendi, M. G. *Angew. Chem., Int. Ed.* **2004**, *43*, 2154.
(30) Swafford, L. A.; Weigand, L. A.; Bowers, M. J. II; McBride, J. R.; Rapaport, J. L.; Watt, T. L.; Dixit, S. K.; Feldman, L. C.; Rosenthal, S. J. *J. Am. Chem. Soc.* **2006**, *128*(37), 12299–12306.
(31) Bawendi, M. G.; Kortan, A. R.; Steigerwald, M. L; Brus, L. E. *J. Chem. Phys.* **1989**, *91*(11), 7282–7289.

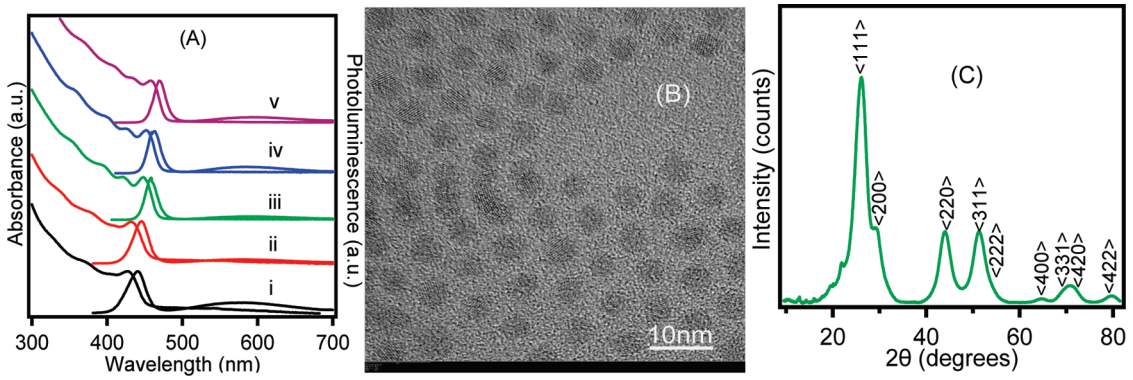

Figure 1. (A) Optical spectra of CdS QDs (i) 4.3, (ii) 4.5, (iii) 4.8, (iv) 5.2, and (v) 5.6 nm; (B) TEM image of 5.3 nm CdS QD; (C) pXRD analysis of a 5.3 nm CdS QD.

reactions were carried out under ambient reaction conditions in a 10 mL borosilicate reaction vessel (4−5 mL reaction volume). The solvent temperature is monitored continuously via a remote infrared (IR) sensor.

For a typical CdS QD reaction,[21] 135.2 mg (0.2 mmol) of cadmium stearate is dispersed into 4 mL of decane, and 0.2 mL (0.2 mmol) of a 1 M TOPS stock solution was added. For reactions carried out in the presence of hexadecylamine (HDA, 0−0.4 mmol) is added to the solution prior to MW heating. The reaction mixture is heated in the microwave reactor from *RT* to a predetermined reaction temperature at 300W and immediately cooled to room temperature *RT* (~1 min). In this manuscript, this reaction protocol will be referred to as zero hold time. The CdS QDs are isolated from the reaction mixture using standard precipitation methods via suspension in a (1:3) toluene/butanol mixture and addition of an excess of methanol to precipitate the entire QD batch. The QD growth behavior appears to be unaffected by the presence or absence of air and therefore all experiments reported herein are carried out without exclusion of ambient air.

Results and Discussion

The formation of 4.3 to 5.6 nm CdS QDs is achieved in the MW within 18 min yielding elliptical, Zinc blende CdS with a 1.2:1 aspect ratio based on analysis of the TEM and pXRD data (Figure 1). By comparison, carrying out the identical reaction using high temperature injection of the precursors in a lyothermal approach does not yield any product on the same time scale (up to 1 h). Conversion efficiency of the precursor to CdS QD is ~25% based on TOPS as the limiting reagent. The experimentally reported size regime is limited in this study, but the range does not reflect an inherent limitation of MW chemistry. The observed experimental limitations herein reflect contributions from the critical energy to initiate QD nucleation and sustain growth by absorption of the MW through the growing QD, wherein the limitations are imposed by the power and temperature limits of the particular MW reactor design.[21] The upper limit for the experimental size range for the current CEM MW configuration utilized in this study reflects maximum microwave power (300W) and maximum temperature limits (280 °C). The smallest size obtainable reflects the necessity to reach at least 180 °C to cleave the TOPS bond. It is expected based on our earlier studies that optimization of concentration, power, pressure, and time may yield smaller CdS samples.

The absorption and PL spectra (Figure 1A) reveal that over the entire size range studied in this manuscript, the CdS QDs exhibit discrete excitonic features in the absorption spectra and strong band edge PL. For the materials prepared in the MW reaction, well-defined higher lying excitonic features in the absorption spectra are clearly observed, which are typically not observed for larger CdS QDs grown by traditional lyothermal methods.[16] The PL defect intensity accounts for < 5% of the total PL intensity in all cases. The size distribution for the samples depends on reaction conditions, but for a 5.3 nm CdS QD prepared from 50 mM CdSA solution carried out at 240 °C, a size distribution of 5.4% (see the Supporting Information, Figure SF1) is observed. For the 5.3 nm CdS sample, clearly resolved ⟨001⟩ lattice fringes are observable (see the Supporting Information, Figure SF2). CdS QDs smaller than 4.5 nm were observed to ablate readily in the TEM thus limiting our ability to utilize TEM analysis to quantify distributions, although low-resolution images confirm distributions in the 5−6% size range. Sizing < 5 nm QDs was carried out by Scherrer broadening analysis of the pXRD, and the relative distributions assumed by analysis of the first exciton full width at half-maximum (fwhm) coupled to the appearance of higher lying excitonic transitions to be consistent with the TEM results. Scherrer broadening analysis on the 5.3 nm CdS QD confirms the use of the pXRD with a size observation from the pXRD of 5.4 nm (Figure 1) and the TEM of 5.3 nm (see the Supporting Information, Figure SF1).

The pXRD pattern for the 5.3 nm CdS QD in Figure 1C exhibits clearly defined reflections at 26.4, 43.9, and 52.1° corresponding to the (111), (220), and (311), which can be fit to the zinc blende ($\bar{F}3m$-T_d^2) crystal lattice. The assignment is confirmed by the lack of intensity for the wurtzite ⟨103⟩ and ⟨102⟩. Although twinning in a QD can give rise to the appearance of a cubic pXRD pattern for a wurtzite crystal, the lack of intensity for the ⟨103⟩ reflection that would appear between the (220) and (311) reflections supports the assignment of the isolation of the metastable cubic phase in Figure 1C. The formation of the metastable phase is not surprising, as it represents the kinetic

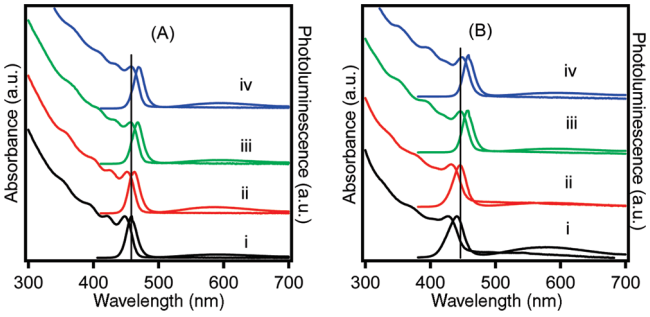

Figure 2. Absorption and photoluminescence spectra of CdS QDs grown (A) in the absence and (B) presence of HDA. All CdS QD samples were grown at 240 °C with a ramp time of 18 min with hold times at the reaction temperature of (i) 0, (ii) 24, (iii) 62, and (iv) 82 min.

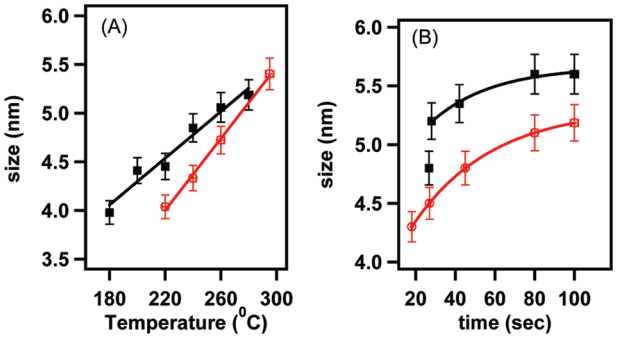

Figure 3. Growth behavior of CdS quantum dots in the MW cavity in the presence (red) and absence (black) of HDA as a function of (A) temperature at zero hold time and (B) carried out at 240 °C, 50 mM CdSA.

structure that is expected to be formed under the highly energetic, rapid nucleation and growth achieved under MW absorption.

Growth. The reaction to form II−VI QDs from metal and chalcogenide monomers is thermodynamically favorable and has been shown to be strongly influenced by the individual activity of the monomers in the solution relative to the monomers on the growing QD surface.[15] As shown previously, the addition of ligands such as alkyl amines, can have a dramatic effect on QD formation by restricting the accessibility of the metal precursor to the growing QD surface thus providing control over QD growth by limiting the precursor addition rate.[6] Likewise, we have shown MW absorption can also impact the growth by controlling the nucleation step through the direct MW absorption of the R_3P-X precursors.[21] Because it is believed that the strength of the R_3P-S limits the sulfur monomer activity in a typical lyothermal reaction, in this study, the competition for controlled growth between direct MW absorption and ligand-dependent monomer controlled growth was explored to determine the optimal growth conditions for CdS.

In the MW, the growth of the CdS QD is governed by the instantaneous nucleation event that occurs upon MW absorption by TOPS, the molecule with the highest static dipole moment. Although the growing QD possesses a dielectric constant that allows MW absorption, the concentration and size of the QD limit its impact on the reaction. As the QD increases in size, the direct absorption into the QD is believed to provide the necessary energy to anneal the CdS QDs, improving overall photophysical properties. Direct MW QD absorption may impact the range over which the CdS QD can be grown at low MW fluence.

The optical properties (exciton fwhm, PL defect intensity) and the size of the isolated CdS QD is observed to strongly depend on the total MW reaction time and the presence (1:1 mol ratio HDA to TOPSe) or absence of hexadecylamine (HDA) (Figure 2). It is clear the observed size of the QD is time-dependent regardless of the presence and absence of HDA; however, the optical quality as measured by the excitonic spectra breadth and spectral detail, as well as photoluminescence appears strongly dependent on the presence or absence of HDA. The narrowest absorption features and lowest PL defect levels are observed for reactions grown in the absence of HDA (Figure 2A). In addition, the CdS QDs are significantly smaller at short reaction times in the presence of HDA implying restricted growth. The restricted growth is consistent with the argument that the presence of HDA appears to impact the accessibility of Cd^{2+} for the growing QD in solution.

A plot of the QD size versus reaction temperature (MW turned off immediately upon reaching the desired temperature) in the presence of HDA (red) and in the absence (black) of HDA is revealing (Figure 3). As the temperature approaches 300 °C, the QD size vs T plot converges (Figure 3A). The data exhibits a linear dependence on T but exhibits different growth rates, as evidenced by the slopes of the lines in Figure 3A. The fits have χ^2 values of 0.033 in the presence of HDA (black) and a value of 0.038 in the reaction lacking HDA (red). No difference is observed for the rate to reach the reaction temperature in the presence or absence of HDA, indicating MW absorption by HDA does not contribute to the reaction rate changes and the observation of delayed growth. For the reaction carried out with zero hold time, it can be concluded that the presence of HDA restricts CdS QD growth when compared to the reaction carried out in the absence of HDA. A similar observation was suggested in the growth control of CdSe in the presence of amines and most likely reflects the reduced activity of the Cd molecular precursors in solution in the presence of HDA, as described previously.[6,18] However, the experimental growth lag in the MW may reflect either growth rate differences or an impact on the initial nucleation step when HDA is present.

The kinetics of growth can be accessed by plotting the QD size vs reaction time at a fixed reaction temperature (240 °C) (Figure 3B). The plot can be fit to an exponential function that demonstrates the same kinetics for QD growth ($\tau = 0.027 \pm 0.04$ s) in the presence and absence of HDA are observed. The χ^2 value for the exponential fit for the reaction lacking HDA (red) is 1.1×10^{-3} and for the reaction containing HDA a χ^2 value of 1.8×10^{-5} (rejecting the 30 s data point) is obtained. The correlation of the kinetics for growth at a fixed temperature implies the growth rate (d_{size}/d_t) is the same regardless of

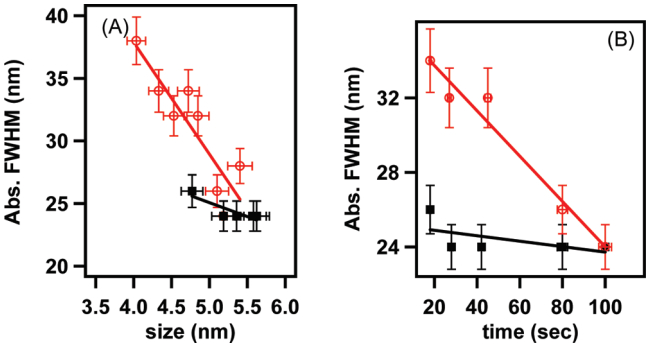

Figure 4. CdS exciton absorption line width (full width half-maximum, fwhm) in the presence (red) and absence (black) of HDA for reactions carried out at 50 mM CdSA (A) for samples at zero reaction time at temperature for variable temperatures, and (B) for samples held at 240 °C for various reaction lengths at a fixed reaction temperature.

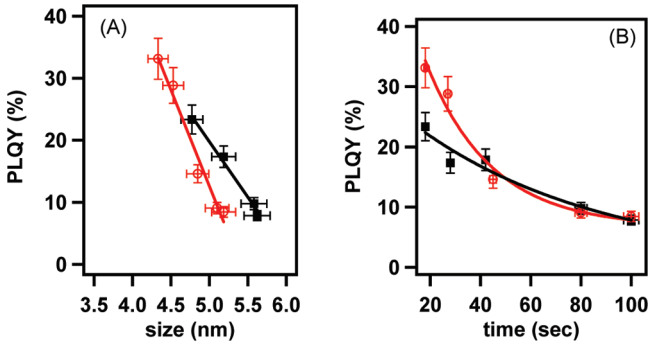

Figure 5. Percent photoluminescence quantum yield (PLQY) in the presence (red) and absence (black) of HDA carried out at 50 mM CdSA (A) for samples at zero reaction time at temperature for variable temperatures, and (B) for samples held at 240 °C for various reaction lengths at a fixed reaction temperature.

monomer activity, and therefore, the smaller initial QD size in the presence of HDA must reflect stabilization of the initial nuclei due to HDA packing, which may lead to an Ostwald ripening process for growth rather than a MW reaction driven process. Above 300 °C, the activation energy of the QD surface or precursors are overcome. Therefore, it is likely the observed size differences at the same temperature for a reaction carried out in the presence and absence of HDA reflects a thermodynamic limitation attributable to the presence of HDA, where the packing of HDA on the growing QD hinders monomer accessibility as has been suggested.[13]

Absorption Properties. The 5.3 nm CdS grown in the absence of HDA yields the sharpest excitonic absorption features reported in the literature to date (Figures 1 and 4).[14,16,32] The dependence of the CdS exciton line width in the absence of HDA is effectively independent of the reaction time or QD size, yielding the narrowest absorption features (fwhm = 24 nm), (Figure 4). It is worth noting that the optical data for this work reflect raw batch QDs isolated by complete precipitation of the CdS QDs from solution by addition of MeOH. In comparison, in the presence of HDA, a strong size and time dependence is observed for the exciton absorption fwhm (38 → 24 nm), only approaching the line width of the non-HDA grown samples for the largest CdS QD size (Figure 4). The narrowing of the line width as a function of time in the presence of HDA can be fit to a linear function with marginal statistics indicating the fit should be treated as a trend line, χ^2 value of 2.2 in the presence of HDA and 2.7 in the absence of HDA. The dramatically larger slope in the presence of HDA at identical reaction temperatures coupled to the observation of initially smaller QDs forming in the MW with a broader size distribution suggests the onset of Ostwald ripening plays a more significant role for QDs gown in the presence of HDA, while in the absence of HDA the MW triggered nucleation has minimal Ostwald ripening contributions. The observation of minimal Ostwald contributions suggest the MW absorption by $R_3P{-}S$ results in a reaction process dominated by MW triggered nucleation, resulting in the rapid depletion of the monomer content in solution.

Photoluminescence Properties. The most remarkable affect of the MW reaction is the improved optical properties for CdS in comparison to lyothermally grown materials. Band edge photoluminescence is observed over the entire size range for the CdS QDs with a narrow PL line width of 18 nm (Figures 1 and 2). The observed PL line width is narrowest for samples grown in the absence of HDA (Figure 2) and only minimal changes in the PL line width or magnitude of the band edge to defect PL intensity is observed as a function of reaction time in the absence of HDA addition. The PLQY for both reaction conditions is size and HDA dependent (Figure 5A), as well as exhibiting a strong dependence on the time at a fixed reaction temperature (Figure 5B). The time dependent data can be fit (χ^2 = 6.7 (red) and 8.5 (black)) to an exponential function with a decline in PLQY as the reaction progresses. The separation of size effects from reaction time effects is difficult as they are intimately related for the larger QD sizes. The observation of passivant dependent and size dependent PLQYs for CdS are not surprising. The reported PL QY for CdS QD varies widely by the method of synthesis. A recent report for CdS preparation within the MW cavity shows a QY of ~2% with a rapid degradation of the PL QY as the reaction times increase.[17] By comparison the lyothermal reaction of CdO, ODE, and sulfur produced a reported QY of 12%.[12]

At long reaction time, the PLQY approaches the same low value for both samples, indicating the time dependence is not due to the presence of HDA (Figure 5B). The time-dependent loss in PLQY is surprising as the line width of the absorption is observed to narrow over the same time domain (Figure 4). A more compelling picture of the affect of QD growth in the MW is gained by comparison of the PLQY for a similar sized CdS grown in the presence and absence of HDA. The data in Figure 5 indicate that the PLQY in reactions grown with HDA is reduced, for example the 5.2 nm CdS grown in the presence of HDA has a PLQY of 8.45%, while the CdS grown in the absence of HDA has a PLQY of 17.8%. The effect of HDA on the reaction is investigated in further

(32) Joo, J.; Bin Na, H.; Yu, T.; Ho Yu, J.; Woon Kim, Y.; Wu, F.; Zhang, J. Z.; Hyeon, T. *J. Am. Chem. Soc.* **2003**, *125*, 11100–11105.

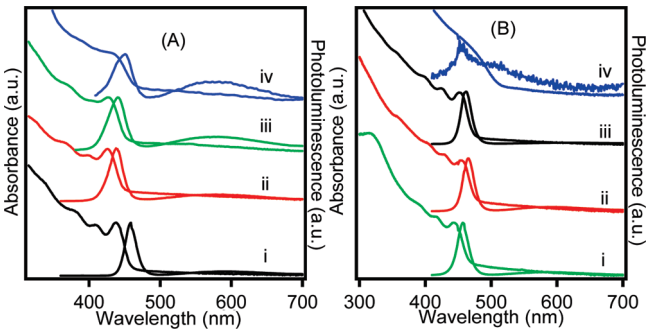

Figure 6. (A) Absorption and PL of CdS is shown as a function of HDA concentration in the reaction mixture. The particles are grown at 240 °C with a ramp time of 18 min and zero hold time time under conditions with (i) no HDA added (0:1 HDA: TOPS), (ii) 0.1 mmol HDA (0.5:1 HDA: TOPS), (iii) 0.2 mmol HDA (1:1 HDA:TOPS), (iv) 0.4 mmol HDA (2:1 HDA:TOPS). (B) The absorption and PL spectra of CdS grown at (i) 3:1, (ii) 2:1, (iii) 1:1, (iv) 1:2 Cd:S mole ratios.

detail below, but it is believed that the variability in PLQY may reflect differences in QD quality under Ostwald ripening conditions, changes in ligand packing densities, or surface reconstruction.[13,33−35] An alternative explanation that may play a role at long times in both reactions is the propensity for CdS to oxidize. Surface oxidation is expected to decrease the PLQY but not lead to sharpening of the absorption features. Therefore, the observation is attributed to time-dependent reconstruction of the QD via Ostwald ripening, which would lead to sharpening of the absorption and potentially loss of PLQY.[36]

Dependence on Monomer and Reactant Concentrations. *HDA Mole Ratio*. It is clear that the presence of HDA strongly influences the properties of CdS growth in the MW cavity. The results of the above experiments imply the Cd monomer activity is influenced by the presence of HDA, and thus impacts either the growth rate by restricting monomer activity or affects the nucleation step. It is likely both steps are influenced as the broadness and slow evolution of the QDs as the reaction temperature increases and the reaction time increases suggest the onset of Ostwald ripening occurs more rapidly in the presence of HDA in the MW when compared to reactions carried out in the absence of HDA. A more in depth analysis of the changes in the materials as a function of HDA is shown in Figure 6A, where the optical spectra as a function of the mole ratio of HDA to TOP at 240 °C (50 mM CdSA) is plotted at zero hold time. The line width of the exciton absorption is broadest (60 nm) for the 2:1 HDA:TOP mole ratio and narrows as the concentration is reduced to 0:1. Although size distribution of the QDs appear to increase with increasing HDA concentration, as evidenced by the loss of the excitonic fine structure as HDA is added to the reaction (Figure 6A), the size of the QD is largely invariant with HDA concentration above a 0.5:1 mol ratio. The observation suggests that the effect is not simply a delay in growth behavior due to monomer restriction but more likely an impact on nucleation and subsequent Ostwald ripening, which occurs following nucleation. The most likely effect is the onset of Ostwald ripening rather than nucleation. The rationale reflects the change in surface ligation and ligand packing that would occur for HDA, which is packed as a highly ordered passivant shell on the QD surface;[33] compared to TOP, which is more disordered. The assumption that the packing of the ligand impacts the QD surface is supported by the observation that the PLQYs are extremely sensitive to the HDA concentration exhibiting a 17.3% PLQY at 0 mmol HDA (0:1 mol ratio HDA to TOPS), 14.3% PLQY at 0.1 mmol (0.5:1 HDA to TOPS), 33.1% at 0.2 mmol HDA (1:1 HDA to TOPS), and 6.4% at 0.4 mmol HDA (2:1 HDA to TOPS).

Influence of the Metal to Chalcogenide Ratio. Further evidence that Ostwald ripening effects are the likely critical difference between the presence and absence of HDA is gained by inspection of the impact of Cd^{2+} mole ratio in the reaction mixture.[6] In Figure 6B, the change in the optical properties as a function of the mole ratio of TOPS to Cd in the absence of HDA shows that the optimum conditions for growth of CdS in the MW requires a 1:1 Cd:S monomer concentration, as evidenced by the optimization of the exciton features and PLQY. For higher S monomer ratios than 1:1 relative to Cd:S, the defect intensity increases, the PLQY is reduced by a factor of 100, and the dispersity of the sample is lost. The loss of the PL features can be interpreted in terms of the reaction in a reaction driven regime, where excess sulfur monomer concentration leads to rapid QD formation with a net increase in vacancy and trap site formation under these experimental conditions.

Conclusion

The observed enhancement of reaction rates for CdS preparation in the MW provides further evidence that selective MW absorption into the TOP-S monomer leads to MW induced activation of the R_3P-S bond and subsequent rapid CdS nucleation and growth. The results are consistent with our earlier reports that R_3P-X, where X is the chalcogenide, completely dominates the initial MW absorption process, leading to nearly instantaneous nucleation and growth.[21] In light of these results, it is instructive to consider the MW-based reaction rates observed for formation of CdS (18 min), CdSe (30 s), and CdTe (15s) carried out under identical conditions. A remarkable correlation exists between the reaction time required for formation of the QD materials and the bond energy for TOP-S (444 ± 8 kJ/mol), TOP-Se (363.6 ± 10.0 kJ/mol), or TOP-Te (279.9 ± 10.0 kJ/mol).[20]

The correlation between experimental reaction times and bond strength supports the assumption that the difficulty in preparation of CdS from TOPS can be interpreted as a pure thermodynamic limitation for the activation of the chalcogenide precursor. The reaction is

(33) Meulenberg, R. W.; Strouse, G. F. *J. Phys. Chem. B* **2001**, *105*, 7438–7445.
(34) Talapin, D. V.; Rogach, A. L.; Kornowski, A.; Haase, M.; Weller, H. *Nano Lett.* **2001**, *1*, 207.
(35) Talapin, D. V.; Rogach, A. L.; Mekis, I.; Haubold, S.; Kornowski, A.; Haase, M.; Weller, H. *Colloids Surf., A* **2002**, *202*, 145.
(36) Jasieniak, J.; Mulvaney, P. *J. Am. Chem. Soc.* **2007**, *129*(10), 2841–2848.

monomer limited by addition of HDA, which leads to a slowing of the reaction dynamics and the observed smaller QDs at identical reaction conditions. The poorer PLQY for HDA may reflect a Cd rich surface due to the presence of HDA. The presence of amines on CdSe QDs has likewise been observed to lower PLQYs.[37] Furthermore, the results strongly support the observation that selective MW absorption can lead to monomer activation in QD reactions. The quality and ease at which CdS can be prepared from TOPS further generalizes the advantages of using selective MW absorption to control nucleation and growth in nanoscale materials.

(37) Landes, C. F.; Braun, M.; El-Sayed, M. A. *J. Phys. Chem. B* **2001**, *105*(43), 10554–10558.

Acknowledgment. The work was supported by funding from the NIH under program EB-R01-00832, the NSF under DMR-0701462, and the Florida-Georgia Lewis Stokes Alliance for Minority Participation fellowship (ALW, II). We thank Ms. Kim Riddle for TEM analysis in the Biological Science Imaging Resource at FSU.

Supporting Information Available: TEM images of CdS quantum dots grown at 5.3 nm showing the dispersity of the particles of 5% (Figure SF1). In addition, a section of this TEM image has been enhanced to the ⟨001⟩ lattices fringes in the highly crystalline CdS materials (Figure SF2) (PDF). This material is available free of charge via the Internet at http://pubs.acs.org.